

BB

CERN LIBRARIES, GENEVA



SCAN-9510118

E4-95-204

SW9542

G.G.Adamian, R.V.Jolos, A.K.Nasirov, A.I.Muminov*

EFFECTS OF SHELL STRUCTURE
AND THE N/Z -RATIO OF A PROJECTILE
ON THE EXCITATION ENERGY DISTRIBUTION
BETWEEN INTERACTING NUCLEI IN DIC

Submitted to «Physical Review C»

*Heavy Ion Physics Department, Institute of Nuclear Physics,
702132 Ulugbek, Uzbekistan

I. INTRODUCTION

A large value for kinetic energy losses is an inherent feature of deep inelastic heavy ion collisions [1,2]. Earlier it was assumed that the relative motion kinetic energy of nuclei, being transformed into intrinsic excitation energy, was distributed between reaction products in approximate proportion to their masses. Recent experiments [3-14], however, have demonstrated that this assumption is incorrect. For example, in the $^{58}\text{Ni}+^{197}\text{Au}$ [3,4], $^{56}\text{Fe},^{74}\text{Ge} + ^{165}\text{Ho}$ reactions [5-12] the excitation energy is about equally divided between the products of the binary reactions for relatively large values of the total kinetic energy losses. In other reactions [3,13,14], the excitation energy distribution is intermediate between equal sharing and sharing proportionate to the fragment masses. In the $^{52}\text{Cr} + ^{208}\text{Pb}$ [13], $^{238}\text{U}+^{124}\text{Sn}$, ^{110}Pd reactions [14] a large part of the excitation energy is concentrated in the light fragments even for a wide range of total kinetic energy loss. These new experiments created a great interest in the problem of kinetic energy dissipation. To reconstruct the primary reaction product yields from the measured evaporation residues, it is important to know how the excitation energy was distributed between the primary fragments.

The fact that thermodynamic equilibrium is not attained as quickly as it was assumed earlier points to the important role of the structure of interacting nuclei even at relatively large kinetic energy losses. The effect of shell structure on the energy dissipation is manifested in the experimental study of the correlation of the total kinetic energy loss with the nucleon exchange between interacting nuclei [2-12,15,16]. The value of the total kinetic energy loss per unit of the charge distribution variance of the products for the $^{208}\text{Pb} + ^{208}\text{Pb}$ reaction is significantly larger than that for the $^{238}\text{U} + ^{238}\text{U}$ reaction [15,16]. The effect of the neutron number variation of the projectile-nucleus on the mass, charge and energy distributions of deep inelastic heavy ion collision products is studied in [17-23].

Interesting results for the yields of neutron-rich nuclei in the incomplete fusion reactions of $^{40,44,48}\text{Ca} + ^{248}\text{Cm}$ were obtained in [18,20]. The observed yields of such elements as Th, U and Pu in the reaction with ^{40}Ca turned out to be two orders of magnitude smaller than

those in the reaction with ^{48}Ca . The cross section of production for elements with masses larger than the target-nucleus mass, however, is of two orders of magnitude larger for the reaction with ^{44}Ca than that for the reaction with ^{48}Ca . From analysis of the N/Z -ratio (N and Z are the neutron and proton numbers) of distribution of secondary nuclides the authors concluded that target-like fragments have small excitation energies. This fact should be taken into account in de-excitation calculations [23]. The difference in excitation energy values in all three $^{40,44,48}\text{Ca} + ^{248}\text{Cm}$ reactions is assumed to be related to the difference in Q_{gg} -values.

The effect of the shell structure and N/Z -ratio of the projectile on the partitioning of excitation energy between interacting nuclei, as well as on mass and charge distributions of the products of deep inelastic heavy ion collisions is studied in [18,20]. It is evident that the analysis of this effect should be based on a microscopic model.

The calculation of frictional coefficients requires explicit formulation of a microscopical model, including the coupling of relative motion to the intrinsic degrees of freedom [24–41]. These models are distinguished by the intrinsic excitations to be considered: collective surface vibrations, giant resonances, non-coherent particle-hole excitations or nucleon exchange between nuclei. It is clear that the structure of excited states and the strength of the coupling of different excitation modes with a relative motion will affect the excitation energy distribution between fragments.

The most commonly used models are those based on the one-body dissipation approach [29,40]. In these models, the friction force is determined by the nucleon exchange through a "window" during nuclear collision [42]. The simplicity of this model [29,40] and its success in describing the kinetic energy loss and the width of the mass (charge) distribution of reaction products are encouraging. The interacting nuclei in the framework of these models, however, are considered in the Fermi-gas approximation, and therefore, the nuclear structure is taken into account only by means of averaging over the ground state energy and parameters of the level density.

One of the advantages of our model [43,44] is that it allows us to explicitly take into

account the effect of the nuclear shell structure on a collision process. A realistic scheme of single-particle states, nucleon separation energies and single-particle matrix elements of nucleon transitions both in each nucleus and from one nucleus to another are constituents of our model. The single-particle approach is improved by the phenomenological account of the residual interaction between nucleons. Another advantage of the model is the possibility of simultaneously considering the particle-hole excitations in each nucleus and the nucleon exchange between nuclei. In the framework of this model, a good agreement with the experimental results has been obtained in describing the dependence of the excitation energy sharing between reaction products on their mass number, and the dependence of the centroid position and variances of the charge and mass distributions on the total kinetic energy loss [43,44].

The basic features of our model are described in Sec. II. In Sec. III, the effects of the projectile shell structure and its N/Z -ratio on excitation energy distribution, centroid position and variance of the charge (mass) distribution for binary reaction products in deep inelastic heavy ion collisions are explored. The role of nucleon exchange and particle-hole excitation mechanisms in the transformation of relative motion kinetic energy into the internal excitation energy of nuclei is studied. Conclusions are given in Sec. IV.

II. MODEL

The model is based on the assumption that colliding nuclei moving along approximately classical trajectories preserve most of their individual properties during the interaction time at the kinetic energies under consideration [1,2,45]. For this reason, the quantum-mechanical consideration of the intrinsic degrees of freedom employs the single-particle approximation with a realistic scheme of the single-particle levels for each nucleus. Each nucleus is described by a potential well (Woods-Saxon type potential) with nucleons in it. The interaction picture can be represented as follows: during the interaction time both potential wells act on the nucleons of each nucleus causing nucleon transitions between single-particle states.

The transitions occurring in each nucleus are particle-hole excitations, while those between partner-nuclei are nucleon exchanges. Thus, in the suggested model, the single-particle mechanism is considered as the main mechanism of excitation and dissipation. The single-particle approach is improved by the phenomenological account of the residual interaction between nucleons. Such effects as excitations of high- and low-lying collective states of the interacting nuclei are neglected. Although contributions to the dissipation could come from easily excited surface vibrations, the adiabaticity of the relative motion with respect to these vibrations decreases their effects.

The total Hamiltonian of a dinuclear system \hat{H} takes the form

$$\hat{H} = \hat{H}_{rel} + \hat{H}_{in} + \hat{V}_{int}. \quad (1)$$

The Hamiltonian of a relative motion

$$\hat{H}_{rel} = \frac{\hat{\mathbf{P}}^2}{2\mu} + \hat{U}(\hat{\mathbf{R}})$$

consists of the kinetic energy operator and a nucleus-nucleus interaction potential $\hat{U}(\hat{\mathbf{R}})$. Here $\hat{\mathbf{R}}$ is the relative distance between the centers of mass of the fragments, $\hat{\mathbf{P}}$ is the conjugate momentum, μ is the reduced mass of the system. The last two terms in (1) describe the intrinsic motion of nuclei and the coupling between relative and intrinsic motions (for details, see [43,44]).

The single-particle Hamiltonian of the dinuclear system $\hat{\mathcal{H}}$ is as follows

$$\hat{\mathcal{H}}(\mathbf{R}(t)) = \sum_{i=1}^A \left(\frac{-\hbar^2}{2m} \Delta_i + \hat{U}_P(\mathbf{r}_i - \mathbf{R}(t)) + \hat{U}_T(\mathbf{r}_i) \right), \quad (2)$$

where m is the nucleon mass, and $A = A_P + A_T$ is the total number of nucleons in the system. The average single-particle potentials of a projectile U_P and a target U_T involve both the nuclear and Coulomb fields.

In the second quantization form the Hamiltonian (2) can be rewritten as

$$\hat{\mathcal{H}}(\mathbf{R}(t)) = \hat{H}_{in}(\mathbf{R}(t)) + \hat{V}_{int}(\mathbf{R}(t)),$$

$$\begin{aligned}
\dot{H}_{in}(\mathbf{R}(t)) &= \sum_i \dot{\varepsilon}_i(\mathbf{R}(t)) \mathbf{a}_i^\dagger \mathbf{a}_i = \sum_{P'} \dot{\varepsilon}_{P'}(\mathbf{R}(t)) \mathbf{a}_{P'}^\dagger \mathbf{a}_{P'} + \sum_T \dot{\varepsilon}_T(\mathbf{R}(t)) \mathbf{a}_T^\dagger \mathbf{a}_T, \\
\dot{V}_{int}(\mathbf{R}(t)) &= \sum_{i \neq j} V_{ij}(\mathbf{R}(t)) \mathbf{a}_i^\dagger \mathbf{a}_j \\
&= \sum_{P' \neq P''} \chi_{P'P''}^{(T)}(\mathbf{R}(t)) \mathbf{a}_{P'}^\dagger \mathbf{a}_{P''} + \sum_{T \neq T'} \chi_{T'T'}^{(P)}(\mathbf{R}(t)) \mathbf{a}_T^\dagger \mathbf{a}_{T'} + \sum_{P,T} \mathbf{g}_{PT}(\mathbf{R}(t)) (\mathbf{a}_P^\dagger \mathbf{a}_T + h.c.).
\end{aligned} \tag{3}$$

Up to the second order in the overlap integral $\langle P|T \rangle$ [46]

$$\begin{aligned}
\varepsilon_{P'}(\mathbf{R}(t)) &= \varepsilon_{P'} + \langle P|U_T(\mathbf{r})|P \rangle, \\
\varepsilon_T(\mathbf{R}(t)) &= \varepsilon_T + \langle T|U_P(\mathbf{r}-\mathbf{R}(t))|T \rangle, \\
\chi_{P'P''}^{(T)}(\mathbf{R}(t)) &= \langle P|U_T(\mathbf{r})|P'' \rangle, \\
\chi_{T'T'}^{(P)}(\mathbf{R}(t)) &= \langle T|U_P(\mathbf{r}-\mathbf{R}(t))|T' \rangle, \\
\mathbf{g}_{PT}(\mathbf{R}(t)) &= \frac{1}{2} \langle P|U_P(\mathbf{r}-\mathbf{R}(t)) + U_T(\mathbf{r})|T \rangle, \dots
\end{aligned} \tag{4}$$

In expression (4) $\varepsilon_{P(T)}$ are the single particle energies of nonperturbed states in the projectile (target) nucleus. These states are characterized by a set of quantum numbers $P \equiv (n_P, j_P, l_P, m_P)$ and $T \equiv (n_T, j_T, l_T, m_T)$ corresponding to the projectile (P) and target (T) nuclei, respectively. The diagonal matrix elements $\langle P|U_T|P \rangle$ ($\langle T|U_P|T \rangle$) define the shifts in single particle energies of the projectile (target) nucleus caused by the target (projectile) mean field. The corresponding nondiagonal matrix elements $\chi_{P'P''}^{(T)}$ ($\chi_{T'T'}^{(P)}$) generate particle-hole transitions in the projectile (target) nucleus. The matrix elements \mathbf{g}_{PT} correspond to the nucleon exchange between reaction partners due to the nonstationary mean field of the dinuclear system. These matrix elements were calculated in the framework of the approach proposed by us [47,48]. The contributions of noninertial recoil effects to the matrix elements are neglected since they are small [35]. The effect of the mean field of one nucleus on states of the other nucleus is taken into account in the second order of perturbation theory:

$$\begin{aligned}
\tilde{\chi}_{P'P''}^{(T)}(\mathbf{R}(t)) &= \chi_{P'P''}^{(T)}(\mathbf{R}(t)) \\
&+ \frac{1}{\hbar} \sum_{P'''} \chi_{P'P'''}^{(T)}(\mathbf{R}(t)) \chi_{P''P''}^{(T)}(\mathbf{R}(t)) \left[\frac{1}{\omega_{P'P''}(\mathbf{R}(t))} + \frac{1}{\omega_{P''P''}(\mathbf{R}(t))} \right],
\end{aligned} \tag{5}$$

$$\begin{aligned}\hat{\chi}_{TT}^{(P)}(\mathbf{R}(t)) &= \chi_{TT}^{(P)}(\mathbf{R}(t)) \\ &+ \frac{1}{h} \sum_{T'} \chi_{TT'}^{(P)}(\mathbf{R}(t)) \chi_{T'T}^{(P)}(\mathbf{R}(t)) \left[\frac{1}{\hat{\omega}_{T'T}(\mathbf{R}(t))} + \frac{1}{\hat{\omega}_{TT'}(\mathbf{R}(t))} \right],\end{aligned}\quad (6)$$

$$\begin{aligned}\hat{g}_{PT}(\mathbf{R}(t)) &= g_{PT}(\mathbf{R}(t)) \\ &+ \frac{1}{h} \sum_{T'} \frac{g_{PT'}(\mathbf{R}(t)) \chi_{TT'}^{(P)}(\mathbf{R}(t))}{\hat{\omega}_{T'P}(\mathbf{R}(t))} + \frac{1}{h} \sum_{P'} \frac{\chi_{P'P}^{(T)}(\mathbf{R}(t)) g_{P'T}(\mathbf{R}(t))}{\hat{\omega}_{P'T}(\mathbf{R}(t))}.\end{aligned}\quad (7)$$

where $\hat{\omega}_{ik}(\mathbf{R}(t)) = [\hat{\varepsilon}_i(\mathbf{R}(t)) - \hat{\varepsilon}_k(\mathbf{R}(t))] / \hbar$.

The explicit consideration of the residual interaction requires cumbersome calculations, but linearization of the two body collision integral simplifies the consideration. In the relaxation time approximation [49] the equation of motion for the single-particle density matrix $\hat{n}(t)$ is

$$i\hbar \frac{\partial \hat{n}(t)}{\partial t} = [\hat{\mathcal{H}}(\mathbf{R}(t)), \hat{n}(t)] - \frac{i\hbar}{\tau} [\hat{n}(t) - \hat{n}^{eq}(\mathbf{R}(t))]\quad (8)$$

where τ is the relaxation time (which will be determined later), $\hat{n}^{eq}(\mathbf{R}(t))$ is a local quasi-equilibrium density matrix at a fixed value of the collective coordinate $\mathbf{R}(t)$:

$$\begin{aligned}\hat{n}_i^{eq}(\mathbf{R}(t)) &= \left[1 + \exp\left(\frac{\hat{\varepsilon}_i(\mathbf{R}(t)) - \lambda_K^{(\alpha)}(t)}{\Theta_K(t)}\right) \right]^{-1}, \\ \Theta_K(t) &= 3.16 \sqrt{(E_K^{*(Z)}(t) + E_K^{*(N)}(t)) / < A_K(t) >},\end{aligned}\quad (9)$$

where $\Theta_K(t)$, $< A_K(t) > = < Z_K(t) > + < N_K(t) >$, $\lambda_K^{(\alpha)}(t)$ and $E_K^{*(\alpha)}(t)$ are the effective temperature, mass number, chemical potential and intrinsic excitation energies for the proton ($\alpha = Z$) and neutron ($\alpha = N$) subsystems of the nucleus K ($K = P, T$), respectively.

The τ_i is calculated in the framework of the theory of quantum liquids [50,51]

$$\begin{aligned}\frac{1}{\tau_i^{(\alpha)}} &= \frac{\sqrt{2}\pi}{32\hbar \varepsilon_{F_K}^{(\alpha)}} \left[(f_K - g)^2 + \frac{1}{2} (f_K + g)^2 \right] \left[(\pi \Theta_K)^2 + (\hat{\varepsilon}_i - \lambda_K^{(\alpha)})^2 \right] \\ &\times \left[1 + \exp\left(\frac{\lambda_K^{(\alpha)} - \hat{\varepsilon}_i}{\Theta_K}\right) \right]^{-1},\end{aligned}\quad (10)$$

where

$$\begin{aligned}\varepsilon_{F_K}^{(Z)} &= \varepsilon_F \left[1 + \frac{2}{3} (1 + 2f') \frac{< N_K > - < Z_K >}{< A_K >} \right], \\ \varepsilon_{F_K}^{(N)} &= \varepsilon_F \left[1 + \frac{2}{3} (1 + 2f') \frac{< N_K > - < Z_K >}{< A_K >} \right]\end{aligned}\quad (11)$$

are the Fermi energies of protons and neutrons ($\epsilon_F=37$ MeV). Here $f_{in}=0.09$, $f'_{in}=0.42$, $f_{ex}=-2.59$, $f'_{ex}=-0.54$, $g=0.7$ are constants of the effective nucleon-nucleon interaction [51]. The finite form of the nucleus has been taken into account by the following expression [51]

$$\begin{aligned} f_k &= f_{in} - \frac{2}{\langle A_K \rangle^{1/3}} (f_{in} - f_{ex}), \\ f'_k &= f'_{in} - \frac{2}{\langle A_K \rangle^{1/3}} (f'_{in} - f'_{ex}). \end{aligned} \quad (12)$$

A formal solution of equation (8) is

$$\begin{aligned} \tilde{n}_i(t) &= \exp\left(\frac{t_0 - t}{\tau_i}\right) \left\{ \tilde{n}_i(t_0) + \sum_k \int_{t_0}^t dt' \int_{t_0}^{t'} dt'' \Omega_{ik}(t', t'') \exp\left(\frac{t'' - t}{\tau_{ik}}\right) [\tilde{n}_k(t'') - \tilde{n}_i(t'')] \right. \\ &\quad \left. + \frac{1}{\tau_i} \int_{t_0}^t dt' \tilde{n}_i^{(eq)}(\mathbf{R}(t')) \exp\left(\frac{t' - t_0}{\tau_i}\right) \right\}, \end{aligned} \quad (13)$$

where

$$\Omega_{ik}(t, t') = \frac{2}{\hbar^2} \text{Re} \left\{ V_{ik}(\mathbf{R}(t)) V_{ki}(\mathbf{R}(t')) \exp \left[i \int_{t'}^t dt'' \tilde{\omega}_{ki}(\mathbf{R}(t'')) \right] \right\}.$$

Equation (13) is solved step by step with the time interval $(t - t_0)$ divided into parts: t_0 , $t_0 + \Delta t$, $t_0 + 2\Delta t$, etc. for $\Delta t < \tau$.

$$\tilde{n}_i(t) = \tilde{n}_i^{(eq)}(\mathbf{R}(t)) \left[1 - \exp\left(\frac{-\Delta t}{\tau_i}\right) \right] + n_i(t) \exp\left(\frac{-\Delta t}{\tau_i}\right), \quad (14)$$

$$n_i(t) = \tilde{n}_i(t - \Delta t) + \sum_k \bar{W}_{ik}(\mathbf{R}(t), \Delta t) [\tilde{n}_k(t - \Delta t) - \tilde{n}_i(t - \Delta t)], \quad (15)$$

where

$$\bar{W}_{ik}(\mathbf{R}(t), \Delta t) = |V_{ik}(\mathbf{R}(t))|^2 \frac{\sin^2\left(\frac{\Delta t}{2} \tilde{\omega}_{ki}(\mathbf{R}(t))\right)}{\left[\frac{\hbar}{2} \tilde{\omega}_{ki}(\mathbf{R}(t))\right]^2}, \quad (16)$$

$n_i(t) = \langle t | \mathbf{a}_i^\dagger \mathbf{a}_i | t \rangle$ is a solution of Eq.(8) without taking into account the residual forces. The dynamic $n_i(t)$ and quasiequilibrium $\tilde{n}_i^{(eq)}(\mathbf{R}(t))$ occupation numbers are calculated at every time step. The initial values of the occupation numbers equal 1 for occupied states and zero for unoccupied ones. The energy of the last complete or partially occupied level ε_i was found to be equal to the nucleon separation energy presented in [52]. The time step Δt used in the calculations is 10^{-22} s.

The present model allows us to calculate the average number of protons $\langle Z_{P(T)} \rangle$ or neutrons $\langle N_{P(T)} \rangle$, their variance σ_Z^2 or σ_N^2 and the intrinsic excitation energies $E_{P(T)}^{*(Z)}(t)$ and $E_{P(T)}^{*(N)}(t)$ for the proton and neutron subsystems of each nucleus:

$$\langle Z_{P(T)} \rangle (t) = \sum_{P(T)}^Z \tilde{n}_{P(T)}(t), \quad (17)$$

$$\langle N_{P(T)} \rangle (t) = \sum_{P(T)}^N \tilde{n}_{P(T)}(t), \quad (18)$$

$$\sigma_{Z(N)}^2(t) = \sum_P^{Z(N)} \tilde{n}_P(t)[1 - \tilde{n}_P(t)], \quad (19)$$

$$E_{P(T)}^{*(\alpha)}(t + \Delta t) = E_{P(T)}^{*(\alpha)}(t) + \sum_{P(T)}^{(\alpha)} [\tilde{\epsilon}_{P(T)}(\mathbf{R}(t)) - \lambda_{P(T)}^{(\alpha)}(\mathbf{R}(t))] [\tilde{n}_{P(T)}(t + \Delta t) - \tilde{n}_{P(T)}(t)], \quad (20)$$

where the top index $Z(N)$ of the sum restricts the summation over proton(neutron) single-particle levels. It is seen from (20) that the fragment excitation energy is calculated step by step along the time scale. Separate summing over the neutron and proton subsystems of each fragment allows us to determine their relative contribution to the excitation energy of the nuclei.

III. MODEL CALCULATIONS

This section is mainly devoted to the study of the deep inelastic heavy ion collisions of $^{34,40,46}\text{Ar} + ^{248}\text{Cm}$, $^{40,44,48,54}\text{Ca} + ^{248}\text{Cm}$, $^{40,48}\text{Ca} + ^{238}\text{U}$ and $^{20,22}\text{Ne} + ^{248}\text{Cm}$. In the framework of our model, we have analyzed the effect of the projectile N/Z -ratio variations on the distribution of the excitation energy between binary products in these reactions. The shifts of the centroid position and variances of charge and mass distributions in these reactions were calculated as well. These distributions are important, for example, in choosing the combinations of reaction partners and their collision energies for synthesis of exotic nuclei. To show the applicability of our model at large nucleus-nucleus interaction times, we have also performed the calculations at a small orbital angular momentum. The relative motion trajectories have been calculated by the same method as in [53,54].

The following notations are used: $R^{P/T} = E_p^*/E_t^*$ is the ratio of the excitation energy of a projectile-like nucleus to a target like nucleus; $R^{ph/ex} = E^{*(ph)}/E^{*(ex)}$ is the ratio of the excitation energy of nuclei produced by particle-hole excitations to that produced by nucleon exchange; $R^{Z/N} = E^{*(Z)}/E^{*(N)}$ is the ratio of the excitation energies of the proton $E^{*(Z)}$ and neutron $E^{*(N)}$ subsystems of the dinuclear system; $\langle \Delta Z_P \rangle = Z_{P^-} - \langle Z_P \rangle$ and $\langle \Delta N_P \rangle = N_{P^-} - \langle N_P \rangle$ are the changes in the mean charge and neutron numbers in the projectile. The excitation energy of each nucleus $E_i^*(i = P, T)$ was calculated by Eq. (20) with summing of the excitation energies of the proton $E_i^{*(Z)}$ and neutron $E_i^{*(N)}$ subsystems. In all figures the abscissa presents the ratios l/l_p , where l_p is the orbital angular momentum for a grazing collision. The experimental total kinetic energy loss scale has been related to the l orbital angular momentum scale.

The calculated values of $R^{P/T}$ (Figures 1a, 2a, 3a, 7a) show that in the $^{34,40,46}\text{Ar} + ^{238}\text{Cm}$, $^{40,44,48,54}\text{Ca} + ^{238}\text{Cm}$, $^{40,48}\text{Ca} + ^{238}\text{U}$ and $^{20,22}\text{Ne} + ^{238}\text{Cm}$ reactions the excitation energy concentrated in the light products is significantly larger than that corresponding to thermodynamic equilibrium. This is seen most clearly in the results of calculations for the reactions with ^{34}Ar and ^{54}Ca . Thus, due to of the short interaction time and the strong difference in the shell structures of the colliding nuclei, a thermodynamic equilibrium in the dinuclear system is not reached.

It is seen (Figures 1, 2, 3, 7) that in all these reactions an increase in the orbital angular momentum leads to an increase in the $R^{P/T}$ and $R^{ph/ex}$ ratios. This means that the relative contribution of particle-hole excitations to the total excitation energy of the dinuclear system also increases with the initial orbital angular momentum l . It is clear that when the relative distance between the interacting nuclei increases (i.e., overlapping of the nuclear densities decreases), the probability of nucleon exchange decreases more rapidly than that of the inelastic excitations of nuclei.

The results of the $R^{ph/ex}$ and $R^{Z/N}$ ratio calculations (see Figures 1, 2, 3 and 7) are sensitive to the value of the N/Z -ratio of the projectile nucleus. From the values of the

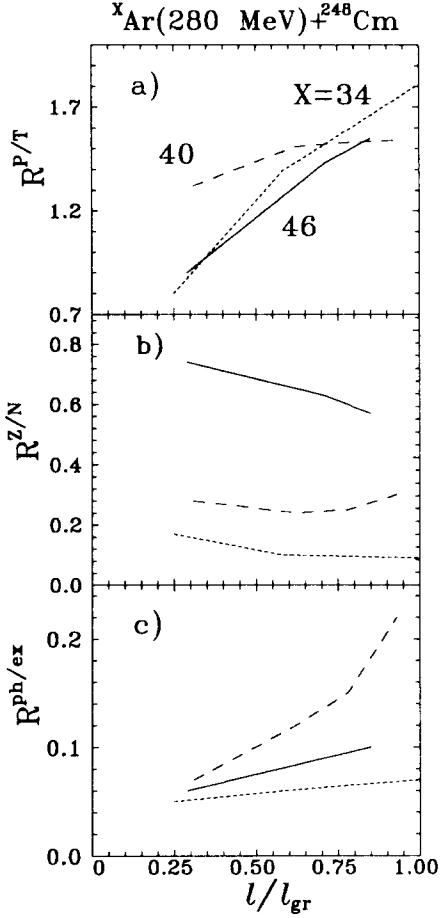


Fig.1. The dependences of the ratios $R^{P/T}$ (a), $R^{Z/N}$ (b) and $R^{ph/ex}$ (c) on l/l_{gr} ($l_{gr} = l_{grazing}$) for the ${}^X\text{Ar}+{}^{248}\text{Cm}$ reactions: $X=34$ (dotted line); $X=40$ (dashed line); $X=46$ (solid line).

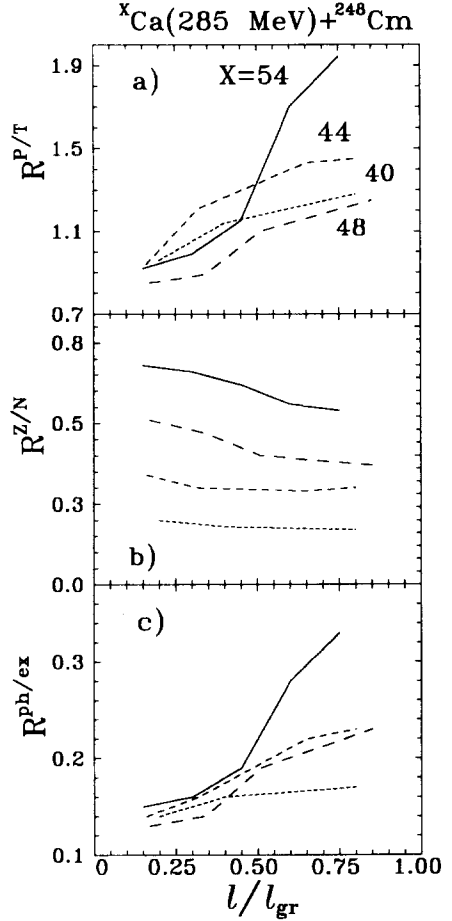


Fig.2. The same as in Fig.1, but for the ${}^X\text{Ca}+{}^{248}\text{Cm}$ reactions: $X=40$ (dotted line); $X=44$ (short dashed line); $X=48$ (long dashed line); $X=54$ (solid line).

$R^{ph/ex}$ ratio one can conclude that nucleon exchange is the main mechanism of kinetic energy dissipation. Comparison of the values of $R^{ph/ex}$ and $R^{Z/N}$ shows that with increasing

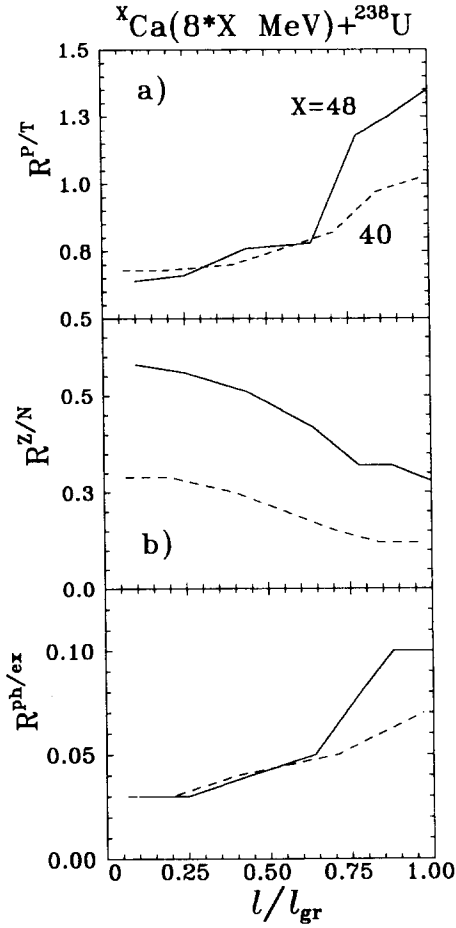


FIG. 3. The same as in Fig.1, but for the ${}^X\text{Ca}+{}^{238}\text{U}$ reactions: $X=40$ (dashed line); $X=48$ (solid line).

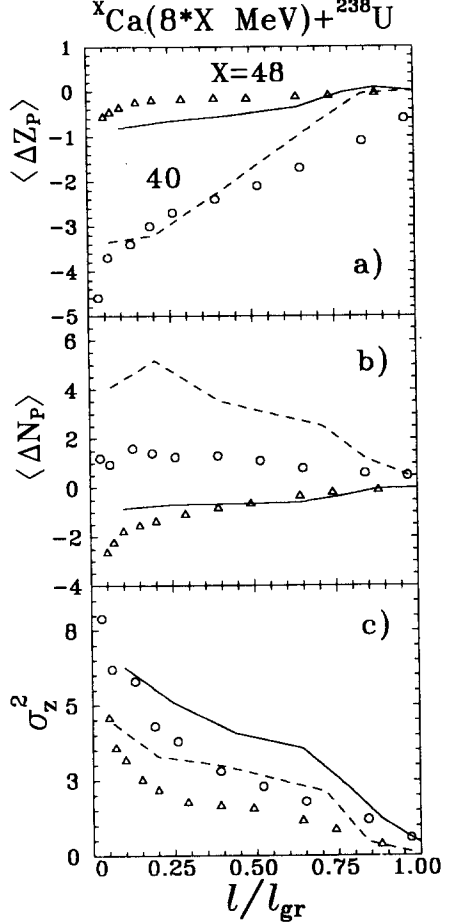


FIG. 4. The change in the mean charge $\langle \Delta Z_P \rangle$ (a) and neutron $\langle \Delta N_P \rangle$ (b) number of the projectile-nucleus and the charge variance σ_Z^2 for the ${}^X\text{Ca}+{}^{238}\text{U}$ reactions as a function l/l_{gr} : the dashed ($X=40$) and solid ($X=48$) lines are results of the calculations and the circles ($X=40$) and triangles ($X=48$) are the experimental data [17].

projectile mass number, the contribution of the proton subsystem to the total excitation energy increases and becomes comparable to that of neutron exchange (Fig. 1b, 2b, 3b and 7b). This enhancement of the role of the proton subsystem in the dissipation process with the increasing projectile N/Z ratio is attributed to the increase in the proton separation energy. As a result, the intensity and direction of the proton (neutron) transfer (Fig. 4a, 4b, 5a, 5b, 6a, 6b, 8a and 8b) between the fragments of the dinuclear system are changed.

The increase in the separation energy means that the proton Fermi level in the projectile with the larger N/Z ratio is deeper than in a projectile with a smaller N/Z . A large difference between the Fermi levels of interacting fragments can increase the number of transferred protons from the target to the projectile. Application of a heavy isotope as a projectile increases the difference between the last filled proton level of the projectile nucleus and first unfilled level of the target nucleus. As a result, the average excitation energy per proton transfer between a heavier projectile isotope and the target nucleus will be larger than that between a lighter projectile and the same target. This effect appears as an increase in the mean energy of the proton subsystem displayed in the increase in $R^{Z/Z}$ (Fig. 1b, 2b, 3b, 7b) and $R^{ph/p,n}$ (Fig. 1c, 2c, 3c, 7c) ratios. The contribution of the proton particle hole excitation energy in the nuclei to the shared total excitation energy will be significant at large values of the orbital angular momentum. As follows from our results, the sharing of the total excitation energy between reaction partners and the distribution of the shared excitation energy between the proton and neutron subsystems of the nucleus should be correctly taken into account in calculating of the pre-equilibrium nucleon yields.

In Figures 4a, 4b, 5a, 5b, 6a, 6b, 8a and 8b the changes of the mean value of proton ($\langle \Delta Z_p \rangle$) and neutron ($\langle \Delta N_p \rangle$) numbers in projectile-like fragments of the $^{40,48}\text{Ca} + ^{238}\text{U}$, $^{34,40,46}\text{Ar} + ^{248}\text{Cm}$, $^{40,44,48,54}\text{Ca} + ^{248}\text{Cm}$ and $^{20,22}\text{Ne} + ^{248}\text{Cm}$ reactions, as functions of l/l_{gr} are presented. The change in the $\langle \Delta Z_p \rangle$ and $\langle \Delta N_p \rangle$ decreases with increasing l because of a reduction in the overlap of nuclei. From Table I and Figures 4a, 4b, 5a, 5b, 6a, 6b, 8a and 8b the sensitivity of $\langle \Delta Z_p \rangle$ and $\langle \Delta N_p \rangle$ to the proton and neutron separation energies is seen. In Fig. 4a, 4b, our results are compared with the experimental

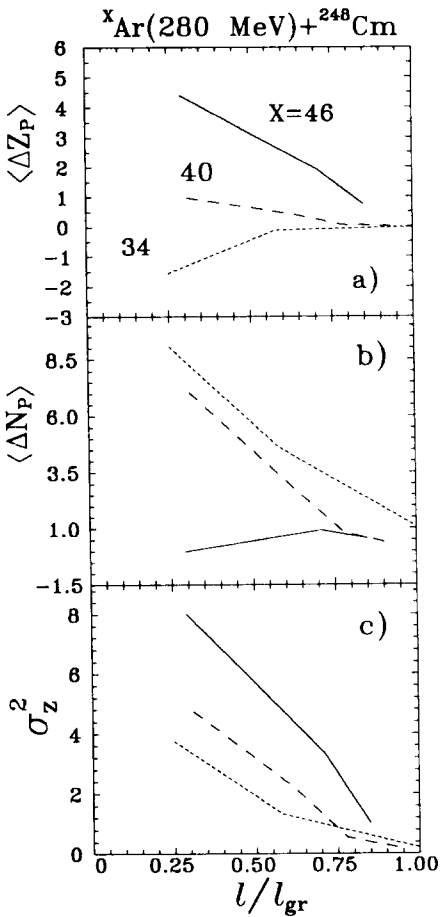


FIG. 5. The same as in Fig.4, but for the ${}^X\text{Ar} + {}^{248}\text{Cm}$ reactions: X=34 (dotted line); X=40 (dashed line); X=46 (solid line).

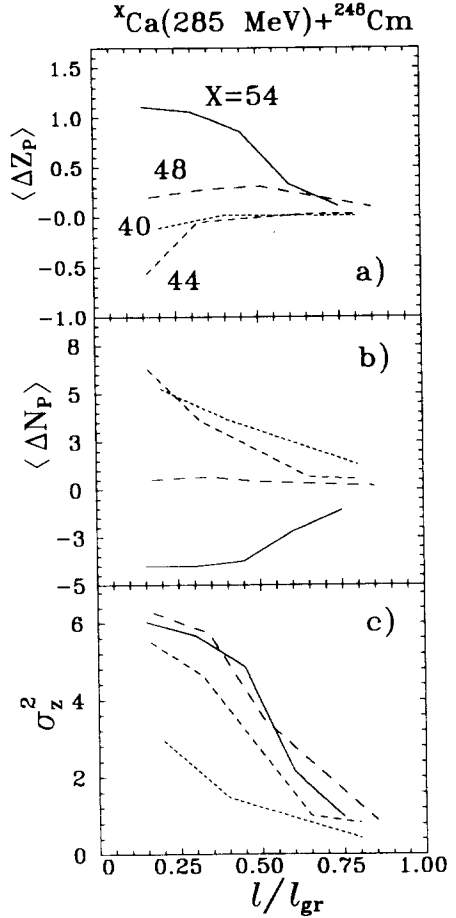


FIG. 6. The same as in Fig.4, but for the ${}^X\text{Ca} + {}^{248}\text{Cm}$ reactions: X=40 (dotted line); X=44 (short dashed line); X=48 (long dashed line); X=54 (solid line).

data for $\langle \Delta Z_P \rangle$ and $\langle \Delta N_P \rangle$ for secondary products of the ${}^{40,48}\text{Ca} + {}^{238}\text{U}$ reactions from [17]. Our results correspond to the primary products. According to our calculations, in

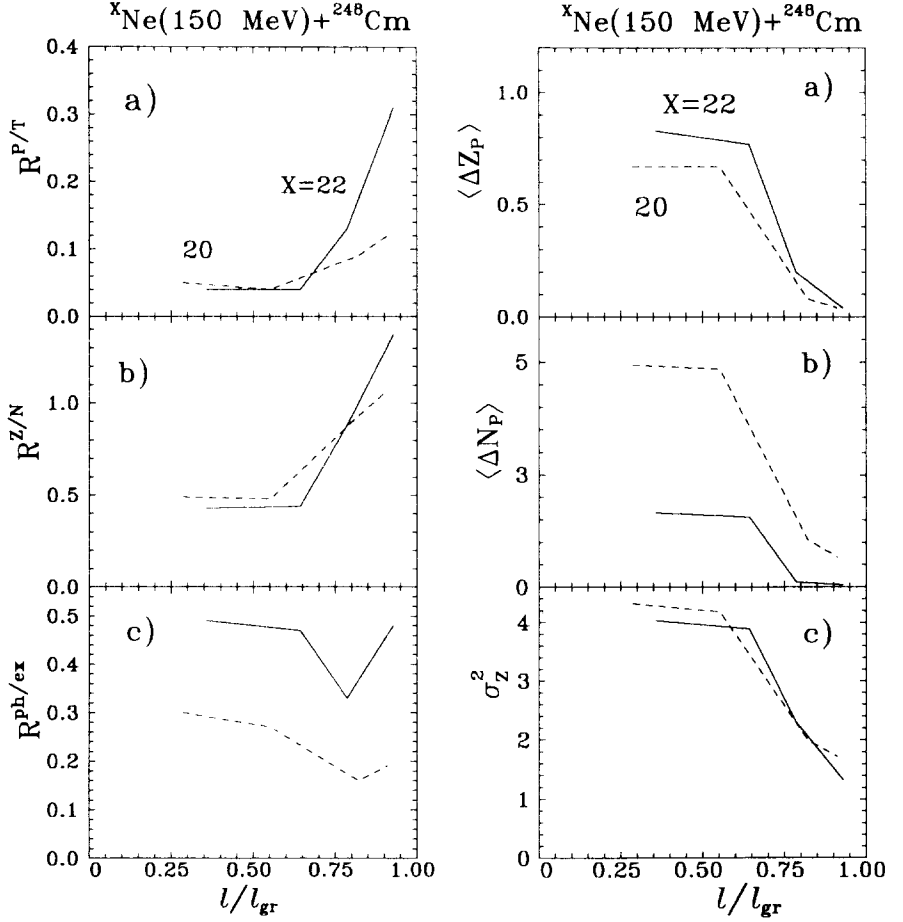


FIG. 7. The same as in Fig.1, but for the ${}^X\text{Ne}+{}^{248}\text{Cm}$ reactions: $X=20$ (dashed line); $X=22$ (solid line).

FIG. 8. The same as in Fig.4, but for the ${}^X\text{Ne}+{}^{248}\text{Cm}$ reactions: $X=20$ (dashed line); $X=22$ (solid line).

the ${}^{40,44}\text{Ca}+{}^{248}\text{Cm}$ reactions, the centroid of the charge distribution moves to increase the charge asymmetry in agreement with the experimentally observed increase in the yields of

Table 1. The proton (S_p) and neutron (S_n) separation energies of Ne, Ar, Ca,

$$S_p = -7.62 \text{ (}^{238}\text{U)}, -7.13 \text{ (}^{248}\text{Cm)}; S_n = -6.15 \text{ (}^{238}\text{U)}, -6.21 \text{ (}^{248}\text{Cm)} \text{ [52].}$$

Element	Ne		Ar			Ca			
A	20	22	34	40	46	40	44	48	54
S_p (MeV)	-12.85	-15.27	4.67	-12.53	-18.51	-8.33	-12.17	-15.81	-22.00
S_n (MeV)	-16.87	-10.36	-17.07	-9.87	-7.22	-15.64	-11.13	-9.94	-5.51

nuclides with masses greater than the mass of the target-nucleus [18,20]. In the reaction with ^{48}Ca , the charge distribution centroid is shifted to decrease the charge asymmetry, which also agrees with the increase in the experimentally observed [18,20] yields of nuclides with masses smaller than the mass of the target-nucleus. Unfortunately, for some characteristics of the reactions the experimental data are not complete.

IV. CONCLUSION

These theoretical results show that the shell structure and the N/Z -ratio of the projectile strongly affect the excitation energy sharing between fragments and the mass (charge) distribution of reaction products in deep inelastic heavy ion collisions. For strongly asymmetric combinations, such as $^{20,22}\text{Ne} + ^{248}\text{Cm}$, $^{34,40,46}\text{Ar} + ^{248}\text{Cm}$, $^{40,48}\text{Ca} + ^{238}\text{U}$ and $^{40,44,48,54}\text{Ca} + ^{248}\text{Cm}$, the excitation energy is about equally shared between the products of the binary reactions. It should be noted that in all these reactions the ratio of the excitation energy of the projectile-like nucleus to that of the target-like nucleus decreases with the initial orbital angular momentum. The contribution of the proton exchange to the total excitation energy increases with the neutron number in the projectile nucleus and becomes comparable to the contribution from the neutron exchange. The nucleon exchange between interacting fragments is the main mechanism of the relative motion kinetic energy dissipation. The relative contribution of particle-hole excitations (mainly protons) to the excitation energy of nuclei also increases with the initial orbital angular momentum.

Our calculations show that the excitation energy of heavy products of the reactions should not be large. Therefore, the probability of particle evaporation from heavy fragments should be small. The authors of the experimental work [18,20] came to the same conclusion on the basis of the narrow form of isotope distributions. For practical purposes, knowledge about the excitation energy distribution between fragments can be used to reconstruct primary reaction product yields [23].

ACKNOWLEDGMENTS

We are grateful to Dr. N.V. Antonenko for fruitful discussions which stimulated the writing of this paper. We wish to thank Dr. F. Akilov, Dr. Zh. Kurmanov and Ms. Ann Schaeffer for their effort in preparing of this manuscript. The authors (G.G.A., R.V.J. and N.A.K.) are grateful to the International Science Foundation for financial support under Grant N RFJ 000 and the Russian Foundation of Fundamental Research (Grant N 95 02 05684).

REFERENCES

- [1] V.V. Volkov, Phys. Rep. **44**, 93 (1978)
- [2] W.U. Schröder and J.R. Huizenga, In: Treatise on Heavy-Ion Science, D.A. Bromley (ed.), Vol.2, p. 115 New York: Plenum Press (1984)
- [3] J. Toke and W.U. Schröder, Annu. Rev. Nucl. Part. **42**, 401, (1992)
- [4] R. Vandenbosh, A. Lazzarini, D. Leach, D.-K. Lock, A. Ray, and A. Seamster, Phys. Rev. Lett. **52**, 1964 (1984)
- [5] T.C. Awes, R.L. Ferguson, R. Novotny, F.E. Obenshain, F. Plasil, S. Pontoppidan, V. Rauch, G.R. Young, and H. Sann, Phys. Rev. Lett. **52**, 251 (1984)
- [6] D.R. Benton, H. Breuer, F. Khazaie, K. Kwiatkowski, V. Viola, S. Bradley, A.C. Mignerey, and A.P. Weston-Dawkes, Phys. Rev. **C38**, 1207 (1988)
- [7] J. Toke, W.U. Schröder, and J.R. Huizenga, Phys. Rev. **C40**, R1577 (1989)
- [8] D. Pade, W.U. Schröder, J. Toke, J.L. Wile, and R.F. de Souza, Phys. Rev. **C43**, 1288 (1991)
- [9] R. Pfaneta, K. Kwiatkowski, S.H. Zhou, V.E. Viola, H. Breuer, M.A. McMahan, J. Randrup, and A.C. Mignerey, Phys. Rev. **C39**, R1197 (1989)
- [10] R. Pfaneta, K. Kwiatkowski, S.H. Zhou, V.E. Viola, H. Breuer, M.A. McMahan, W. Kehoe, and A.C. Mignerey, Phys. Rev. **C41**, 912 (1990)
- [11] K. Kwiatkowski, R. Pfaneta, S.H. Zhou, V.E. Viola, H. Breuer, M.A. McMahan, and A.C. Mignerey, Phys. Rev. **C41**, 958 (1990)
- [12] J. Toke, R. Pfaneta, W.U. Schröder, and J.R. Huizenga, Phys. Rev. **C44**, 390 (1991)
- [13] H. Keller, B. Bellwied, K. Lützenkirchen, J.V. Kratz, W. Bröchle, H. Gäggler, K.J. Moody, M. Schädel, and G. Wirth, Z. Phys. **A328**, 255 (1987)

- [14] G. Beier, J. Friese, W. Henning, P. Kienle, H.J. Körner, W. Wagner, W.A. Mayer, and W. Mayer, *Z. Phys.* **A336**, 217 (1990)
- [15] T. Tanabe, R. Bock, M. Dakowski, A. Gobbi, H. Samt, H. Stelzer, U. Lynen, A. Olmi, and D. Pelte, *Nucl. Phys.* **A342**, 191 (1980)
- [16] K.D. Hildenbrand, H. Freiesleben, F. Pühlhofer, W.F.W. Schneider, R. Bock, D.V. Harrach, and H.J. Specht, *Phys. Rev. Lett.* **39**, 1065 (1977); *Z. Phys.* **A292**, 171 (1979)
- [17] R.T. de Souza, W.U. Schröder, J.R. Huizenga, J. Töke, J.L. Wile, and S.S. Datta, *Phys. Rev.* **C39**, 114 (1989)
- [18] D.C. Hoffman, M.M. Fowler, W.R. Daniels, H.R. von Gunten, D. Lee, K.J. Moody, K.E. Gregorich, R. Weich, G.T. Seaborg, W. Brüchele, M. Brügger, H. Gäggeler, M. Schädel, K. Summerer, G. Wirth, Th. Blaich, G. Herrman, N. Hildenbrand, J.V. Kratz, M. Lerch, and N. Trautmann, *Phys. Rev.* **C31**, 1763 (1986)
- [19] R.T. de Souza, J.R. Huizenga, and W.U. Schröder, *Phys. Rev.* **C37**, 1901 (1988)
- [20] A. Türler, H.R. von Gunten, J.D. Louba, D.C. Hoffman, D.M. Lee, K.E. Gregorich, D.A. Bennett, R.M. Chasteler, C.M. Gannett, H.L. Hall, R.A. Henderson, and M.J. Nurmia, *Phys. Rev.* **C46**, 1361 (1992)
- [21] J.L. Wile, S.S. Datta, W.U. Schröder, J. Töke, D. Pade, S.P. Baldwin, J.R. Huizenga, B.M. Quedman, R.T. de Souza, and B.M. Szabo, *Phys. Rev.* **C47**, 2135 (1993)
- [22] C.H. Dasso, G. Pollaro, and A. Winther, *Phys. Rev. Lett.* **73**, 1907 (1994)
- [23] N.V. Antonenko, E.A. Cherepanov, A.S. Hijnov, and M.V. Mebel, *J. Alloys and Compounds.* **213/214**, 460 (1994)
- [24] H. Hofmann and P.J. Siemens, *Nucl. Phys.* **A257**, 165 (1976); **A275**, 464 (1977)
- [25] G. Bertsch and R. Schaeffer, *Nucl. Phys.* **A277**, 509 (1977)

- [26] D.H.E. Gross and H. Kalinowski, Phys. Reports **45**, 175 (1978)
- [27] K. Sato, S. Yamaji, K. Harada, and S. Yoshida, Z. Phys. **A290**, 119 (1979)
- [28] P.J. Johansen, P.J. Siemens, A.S. Jensen, and H. Hofmann, Nucl. Phys. **A288**, 152 (1977)
- [29] J. Randrup, Nucl. Phys. **A307**, 319 (1978); **A327**, 190 (1979); **A383**, 168 (1982)
- [30] S. Ayik, Z. Phys. **A292**, 257 (1979)
- [31] D. Agassi, C.M. Ko, and H.A. Weidenmüller, Ann. of Physics **117**, 407 (1979)
- [32] J. Bartel and H. Feldmeier, Z. Phys. **A297**, 333 (1980)
- [33] S. Pal and N.K. Ganguly, Nucl. Phys. **A370**, 175 (1981)
- [34] S. Ayik and W. Nörenberg, Z. Phys. **A309**, 121 (1982)
- [35] S. Yamaji and A. Iwamoto, Z. Phys. **A313**, 161 (1983)
- [36] H. J. Krappe, Nucl. Phys. **A505**, 117 (1989) 139 (1986)
- [37] F. Catara and E.G. Lanza, Nucl. Phys. **A451**, 299 (1986)
- [38] M. Baldo, A. Rapisarda, R.A. Broglia, and A. Winther, Nucl. Phys. **A472**, 333 (1987)
- [39] Z. He, P. Rozmej, and W. Nörenberg, Nucl. Phys. **A473**, 342 (1987)
- [40] H. Feldmeier, Rep. Prog. Phys. **50**, 1 (1987)
- [41] R.V. Jolos, R. Schmidt, and J. Teichert, Nucl. Phys. **A249**, 139 (1981)
- [42] J. Blocki, Y. Bunch, J.R. Nix, J. Randrup, M. Robel, A.J. Sierk, and W.J. Swiatecki, Ann. of Phys. **113**, 330 (1978)
- [43] G.G. Adamian, R.V. Jolos, and A.K. Nasirov, Z. Phys. **A347**, 203 (1991)
- [44] G.G. Adamian, N.V. Antonenko, R.V. Jolos, and A.K. Nasirov, Phys. Part. Nucl. **A25**, 583 (1991)

- [45] V.V. Volkov, Intern. School-Seminar on Heavy Ion Physics, Dubna, 1986, D7-87-68
Dubna, p. 528 (1987); Proc. of the 6th Intern. Conf. on Nuclear Reactions Mechanisms,
ed. E.Gadioli, Varanasi, p. 39 (1991)
- [46] N.V. Antonenko and R.V. Jolos, Z. Phys. **A338**, 123 (1991)
- [47] G.G. Adamian, R.V. Jolos, and A.K. Nasirov, Sov. J. Nucl. Phys. **55**, 660 (1992)
- [48] G.G. Adamian, N.V. Antonenko, R.V. Jolos, and A.K. Nasirov, Nucl. Phys. **A551**, 321
(1993)
- [49] H.S. Köhler, Nucl. Phys. **A343**, 315 (1980); **A378**, 181 (1982)
- [50] D. Pines and P. Nozières, The theory of quantum liquids, Benjamin, NY (1966)
- [51] A.B. Migdal, Theory of the finite Fermi system and property of the atomic nucleus,
Moscow, Nauka (1983)
- [52] A.M. Wapstra and G. Audi, Nucl. Phys. **A565**, 1 (1993)
- [53] R. Schmidt, G. Wolschin, and V.D. Toneev, Nucl. Phys. **A311**, 217 (1978)
- [54] R. Schmidt, Part. & Nucl. **13**, 1203 (1982)

Received by Publishing Department
on April 28, 1995.

Влияния оболочечной структуры и N/Z -отношения в налетающем ядре на распределение энергии возбуждения между взаимодействующими ядрами в глубоконеупругих столкновениях

Рассмотрены глубоконеупругие столкновения стабильных и радиоактивных снарядов с тяжелыми мишенями. Исследованы влияния оболочечной структуры и N/Z -отношения в налетающем ядре на распределение энергии возбуждения между продуктами, положения максимумов и величины дисперсий зарядовых и массовых распределений бинарных продуктов реакции. Исследована роль нуклонного обмена и частично-дырочных возбуждений в трансформации кинетической энергии относительного движения во внутреннюю энергию ядер. Показано, что изменение массового числа налетающего ядра приведет к значительным изменениям как в распределении энергии возбуждения между фрагментами, так и в зарядовом (массовом) распределении продуктов реакции. Процесс обмена нуклонами между взаимодействующими ядрами является основным механизмом диссипации кинетической энергии.

Работа выполнена в Лаборатории теоретической физики им. Н.Н.Боголюбова ОИЯИ.

Препринт Объединенного института ядерных исследований. Дубна, 1995

Effects of Shell Structure and the N/Z -Ratio of a Projectile on the Excitation Energy Distribution between Interacting Nuclei in DIC

Deep inelastic collisions of stable and radioactive projectiles with heavy targets are considered. The effects of shell structure and the N/Z -ratio of a projectile on the excitation energy distribution between interacting nuclei, and on the centroid position and variance of the charge (mass) distribution of binary reaction products are explored. The role of nucleon exchange and particle-hole excitation mechanisms in the transformation of relative motion kinetic energy into the internal excitation energy of nuclei is studied. It is shown that a change in the mass number of the projectile-nucleus causes a sufficient change both in the sharing of the excitation energy between fragments and the charge (mass) distribution of reaction products. The nucleon exchange process between interacting nuclei is the main mechanism of dissipation.

The investigation has been performed at the Bogoliubov Laboratory of Theoretical Physics, JINR.

Preprint of the Joint Institute for Nuclear Research. Dubna, 1995

Макет Т.Е.Попеко

Подписано в печать 31.05.95
Формат 60×90/16. Офсетная печать. Уч.-изд.листов 1,67
Тираж 370. Заказ 48233. Цена 1002 р.

Издательский отдел Объединенного института ядерных исследований
Дубна Московской области